

# Gasoline HCCI engine with DME (Di-methyl Ether) as an Ignition Promoter

---

Kitae Yeom, Jinyoung Jang, Choongsik Bae

## Abstract

Homogeneous charge compression ignition (HCCI) combustion is an attractive way to lower carbon dioxide (CO<sub>2</sub>), nitrogen oxides (NO<sub>x</sub>) emission and to allow higher fuel conversion efficiency. However, HCCI engine has inherent problem of narrow operating range at high load due to high in-cylinder peak pressure and consequent noise. To overcome this problem, the control of combustion start and heat release rate is required. It is difficult to control the start of combustion because HCCI combustion phase is closely linked to chemical reaction during a compression stroke.

The combination of variable valve timing (VVT) and gas fuel injection of high cetane number was chosen as the most promising strategy to control the HCCI combustion phase in this study. Regular gasoline was injected at intake port as main fuel, while small amount of di-methyl ether (DME) was also injected directly into the cylinder as an ignition promoter for the control of ignition timing. Different intake valve timings were tested for combustion phase control. Regular gasoline was tested for HCCI operation and emission characteristics with various engine conditions. This paper investigates the steady-state combustion characteristics of the HCCI engine with VVT, to find out its benefits in exhaust gas emissions. With HCCI operation, higher internal exhaust gas recirculation (EGR) rate and the longer combustion duration reduced NO<sub>x</sub> emissions. However, hydrocarbon (HC) emission is relatively higher than that under spark-ignition combustion.

## 1. Introduction

The homogeneous charge compression ignition (HCCI) engine allows lower nitrogen oxides (NO<sub>x</sub>) engine-out emissions and higher efficiency than conventional SI engine due to lean burn characteristics of auto-ignited homogeneous charge. Thus, HCCI engine attracted many researchers and car manufacturers. However, several technical problems are facing HCCI engine to be applied to production. Peak pressure rise is so large that engine noise increases at high load. Peak gas temperature is so low as to cause high carbon oxide (CO) and hydrocarbon (HC) emissions at low load [1]. It was reported that boosting with turbocharger could improve the brake mean effective pressure (BMEP) and expand operating range [3, 4]. Exhaust gas recirculation (EGR) is used to control NO<sub>x</sub> emission. A fraction of the exhaust gases are recycled from the exhaust to the intake system. This exhaust gas acts as additional diluents in the unburned gas mixture. Residual gas of a cycle acts the same function at the next cycle, which is called as internal EGR. To control internal exhaust gas recirculation (EGR), EMV and variable valve actuation (VVA) could be used [5 - 7]. Electro magnetic valvetrain (EMV) is future engine concept, where the inlet and exhaust valves

are actuated by a single control unit per valve, consisting of the actuator and sensor. The variable compression ratio (VCR) also becomes a challenging alternative method. VCR is achieved by tilting the upper part of the engine. The higher compression ratio can increase the charge temperature during compression stroke [8].

In most cases of direct injection gasoline engine, the injected fuel impinges onto the cylinder wall or piston crown. These impinged fuels cause a major source of particulate matter (PM) or HC emissions. However, DME vaporizes and ignites easily due to higher vapor pressure [2]. Therefore, DME is suitable to control the start of ignition in a direct injection HCCI engine. DME direct injection HCCI operation has been successfully used in high speed direct injection (HSDI) fuel system [9]. Moreover, DME has also been tested for port injection [10].

The residual gas gives thermal energy to fresh charge for easy ignition [7]. The early intake valve opening allows more residual gas inside the cylinder, because of longer valve overlap than late intake valve opening [11].

In this paper, the feasibility of gasoline fueled HCCI combustion was examined combining VVT and DME direct injection. The effects of various intake valve timings, DME injection timings, DME and gasoline quantities on the NO<sub>x</sub> and HC emissions have been investigated.

## 2. Experimental apparatus

### 2.1 Engine

Figure 1 shows a schematic diagram of the experimental setup. The specifications of engine are given in Table 1. It is a single cylinder, double over head camshaft (DOHC) engine equipped with VVT and DME direct injection system. The engine speed and load are controlled by alternating current (AC) dynamometer. A direct injection spark ignition (DISI) slit injector (Denso) was used to inject DME at constant supply pressure of 50 bar using pressurized nitrogen gas. DISI injector was located

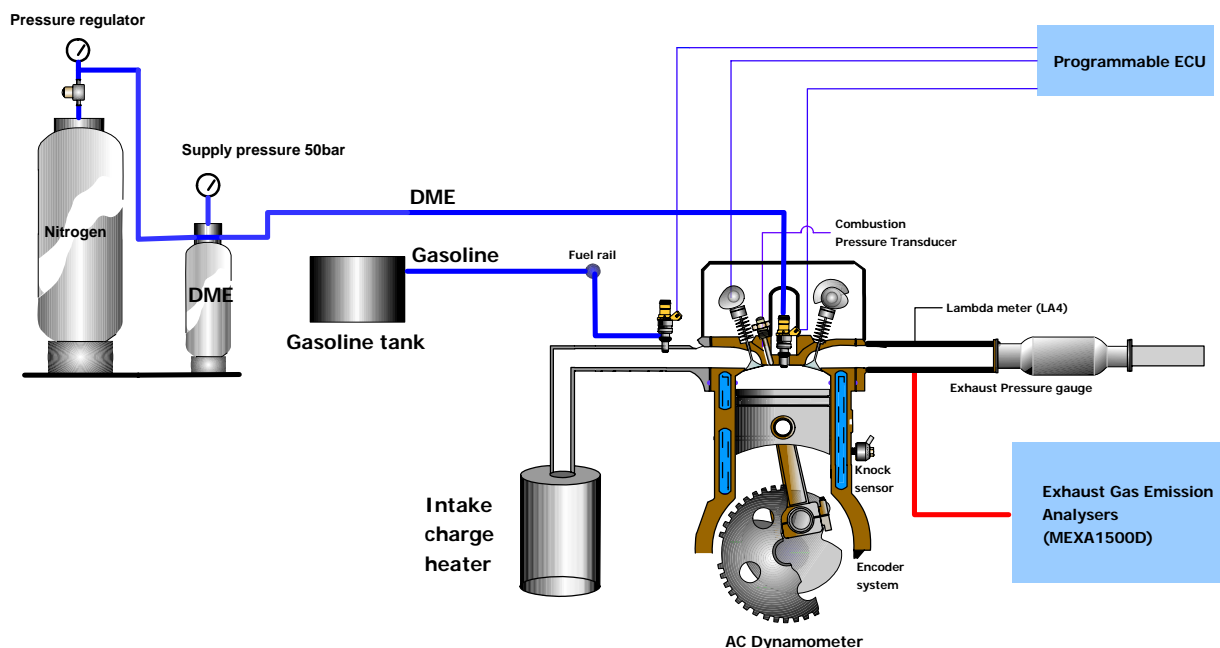


Figure 1 Experimental apparatus

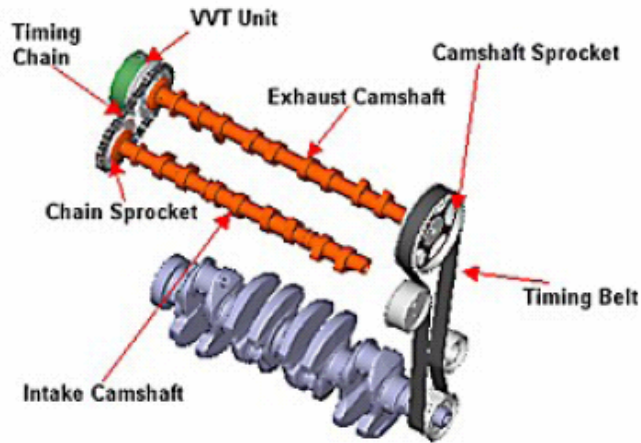


Figure 2 Schematic diagram of VVT

Table 1 Engine specifications

Bore (mm)		82
Stroke (mm)		93.5
Compression ratio		12
Displacement (cc)		494
Intake / Exhaust valve duration		228 / 228
Intake / Exhaust valve lift		8.5 / 8.4
Valve timing (CAD)	Intake Valve Open (ATDC)	-29 ~ 11
	Intake Valve Close (ABDC)	59 ~ 19
	Exhaust Valve Open (BBDC)	42
	Exhaust Valve Close (ATDC)	6
DME injection pressure (bar)		50
DISI injector type		Slit injector

Table 2 Experimental conditions

Engine speed (rpm)		1000
Intake Valve Open timing (CAD)		-29, -19, -9, 1, 11
DME injection timing (CAD)		110, 210, 310, 330, 340
$\lambda_{DME}$		2.59, 2.86, 3.17, 3.50, 4.14, 4.52, 4.96, 5.45, 6.06
$\lambda_{Gasoline}$		1, 1.13, 1.31, 1.56, 1.92, 2.5, 3.16, 3.6
Intake charge temperature ( $^{\circ}C$ )		70
Coolant / Oil temperature ( $^{\circ}C$ )		70 / 70

on spark plug hole. Lubricity enhancer (Infineum R655) of 500 ppm was added to the neat DME to avoid any damage of the fuel injection system.

Figure 2 shows a schematic diagram of the VVT system which can vary intake valve open and close timing freely. The intake valve open timing was varied in the range of 29 crank angle degree (CAD) before top dead center (BTDC) to 11 CAD after top dead center (ATDC), while valve duration was fixed as 228 CAD.

A piezoelectric pressure transducer (Kistler, 6052b) was used for the measurement of in-cylinder pressure. Two piezo-resistive pressure transducers (Kistler, 4045A5) were used for the measurement of intake and exhaust manifold pressures. Two K-type thermocouples were fitted on the intake and exhaust manifold to measure the temperature. A wide band lambda meter (ETAS, LA4) was installed for the measurement of relative air / fuel ratio. Exhaust gases were analyzed with a gas analyzer (Horiba, Mexa 1500d) to measure HC, NO<sub>x</sub>, CO. A data acquisition system (IOtech, Wavebook 512H) was employed to acquire all engine combustion and exhaust gas data. Indicated mean effective pressure (IMEP) and heat release rate were calculated from the cylinder pressure values.

The ignition delay is the period between the start of DME injection and the start of combustion which was identified from a heat-release analysis [12]. The rapid burning angle is the period between the crank angle for 10% mass fraction burned and the crank angle for 90% mass fraction burned [12]. Relative air / fuel ratio is defined as the ratio;  $(A / F)_{\text{actual}} / (A / F)_{\text{stoichiometric}}$ .

## 2.2 Experimental condition

Table 2 shows the main experimental conditions used in this study. Figure 3 shows the intake valve timings and DME injection timings. The engine was run at 1000 rpm for various intake valve timings, DME injection timings and equivalence ratios. Gasoline was injected at intake manifold during exhaust stroke.

## 3. Results and discussion

### 3.1 The effects of Intake valve open timings

Intake valve open (IVO) timing was varied from -29 CAD to 11 CAD when DME injection timing, relative air / gasoline ratio ( $\lambda_{\text{gasoline}}$ ) and relative air / DME ratio ( $\lambda_{\text{DME}}$ ) were fixed at 340 CAD, 3.16, 3.5, respectively.

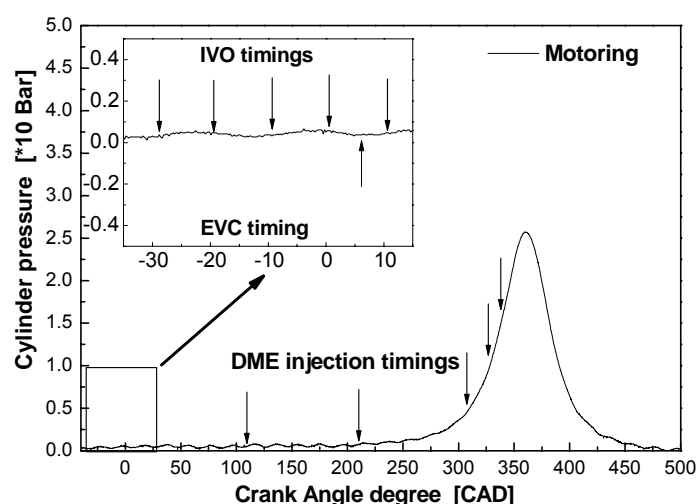


Figure 3 Intake valve timings and DME injection timings

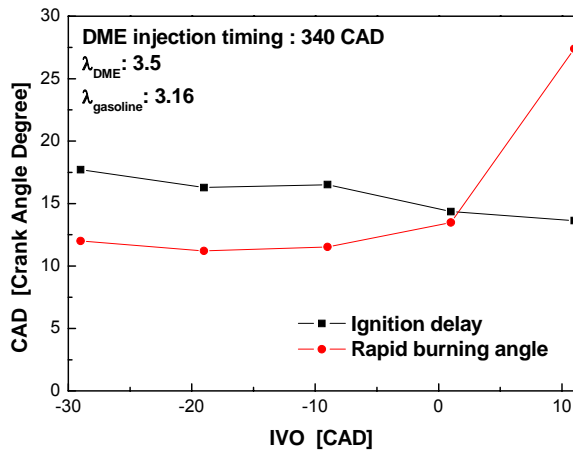


Figure 4 Ignition delay and rapid burning angle as a function of crank angle as IVO timings

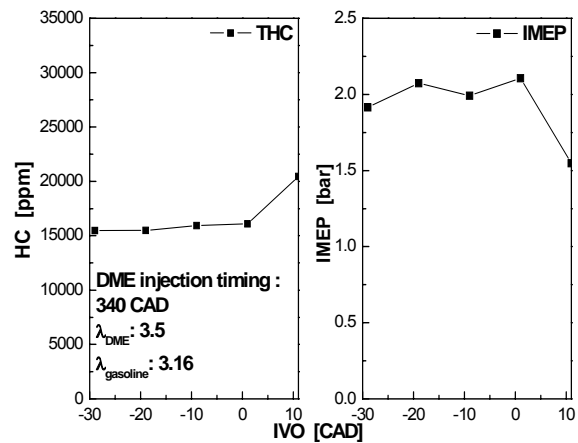


Figure 5 HC emission and IMEP as a function of IVO timings

Figure 4 shows ignition delay and rapid burning angle for various IVO timings. The horizontal axis represents the IVO timing, and the vertical axis represents crank angle degree. It shows that ignition delay was slightly decreased as intake valve timing was retarded. Dilution of the burned gas was the major reason of shorter ignition delay. Internal EGR reduces the ratio of specific heat of the cylinder charge. Because of the reduced ratio of specific heat, in the compressed mixture of fuel and fresh charge temperature gets lower at the end of compression stroke. At -19 CAD of IVO timing, rapid burning angle was shortest among the all valve timing cases. At -9, 1, 11 CAD of IVO timing, rapid burning angle was increased as intake valve timing was retarded. This can be understood by volumetric efficiency. At 11 CAD of IVO timing, volumetric efficiency was 79%. While, at -29 CAD of IVO timing, it was 67.4%.

Figure 5 shows HC emission and IMEP as a function of IVO timings. The horizontal axis represents the IVO timing, and the vertical axis represents HC and IMEP. At 11 CAD of IVO timing, HC was sharply increased by 4500 ppm (25%) and IMEP was 25% lower. The reason of this change is the longer rapid burning angle as shown previously in Figure 4. During the expansion stroke, at 11 CAD of IVO timing, unburned end gas pressure and temperature were much lower than at 1 CAD of IVO timing. Because of the lower end gas temperature and pressure, at 11 CAD of IVO timing, quenching effect was stronger than at 1 CAD of IVO timing. And, at 11 CAD of IVO timing, fuel conversion efficiency was 8.43%. While, at 1 CAD of IVO timing, it was 11.47%. These things imply that a large fraction of unburned fuel was exhausted during exhaust stroke.

### 3.2 The effects of DME injection timings

Ignition delay and rapid burning angle as a function of DME injection timing are shown in Figure 6. The change in rapid burning angle for early injection timings between 110 CAD and 210 CAD was negligible. Injection during this period allows enough time to achieve a well-premixed charge. However, At 110, 210 CAD of DME injection timings, rapid burning angle was 70% longer than after 310 CAD DME injection timings. Increase of rapid burning angle can be explained by the fact that lean

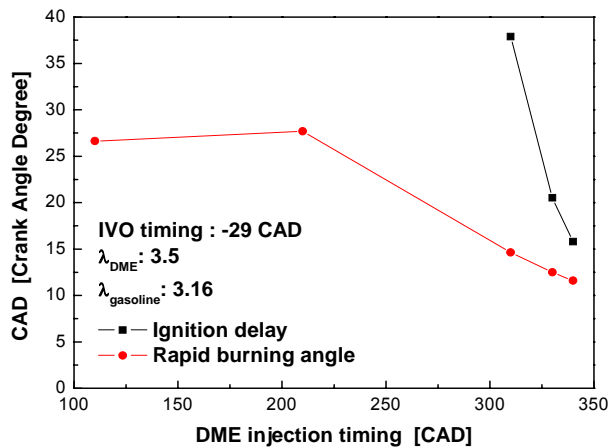


Figure 6 Ignition delay and rapid burning angle as a function of DME injection timings

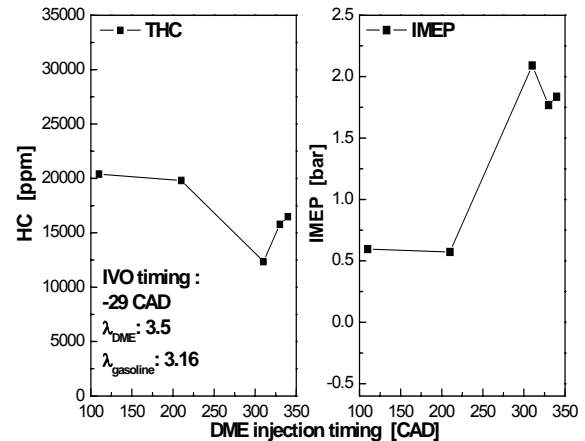


Figure 7 HC emission and IMEP as a function of DME injection timings

homogeneous mixture takes more time to be burned. Rapid burning angle was decreased as DME injection timing is retarded after 210 CAD. Though the rapid burning angle was significantly affected by DME injection timing, the start of combustion was not influenced.

HC emission and IMEP as a function of DME injection timing are shown in Figure 7. The lowest value of HC emission was found at injection timing of 310 CAD. At this crank angle, IMEP was also the highest value among all the cases. This indicates that more fuel was burned in 310 CAD case. This is because ignition delay was decreased as injection timing was retarded. And, the start of combustion occurred near top dead center (TDC). At the early DME injection at 110 CAD and 210 CAD, HC emission was bigger than the cases of the late injections at 310 CAD and 330 CAD. In addition, IMEP was 75% lower than the case of 310 CAD. This is because of slow burning. The combustion temperature is too low for the fuel distributed near cylinder wall to be burned. Exhaust gas temperature was 81.3 °C at 110 CAD of DME injection timing. While, it was 108 °C at 310 CAD of DME injection timing. These things imply that the best IMEP was achieved when DME was injected during compression stroke.

### 3.3 The effects of fuel quantities

To investigate the effect of fuel quantities on gasoline HCCI engine, IVO timing was fixed at 11 CAD, which corresponds to the longest rapid burn duration as shown previously. Because rich operation is limited by rapid combustion pressure rise corresponding to the peak value of heat release rate, longer rapid burn duration can expand rich operation region. DME injection timing was fixed at 310 CAD for best IMEP. The map of total relative air / fuel ratio ( $\lambda_{TOTAL}$ ) of air, gasoline and DME mixture through all the experiment condition is displayed in Figure 8. Considering the stoichiometry of the mixture (gasoline, DME and air),  $\lambda_{TOTAL}$  is described as the following equation.

$$\lambda_{TOTAL} = \frac{\lambda_{gasoline} \lambda_{DME}}{\lambda_{gasoline} + \lambda_{DME}} \quad (1)$$

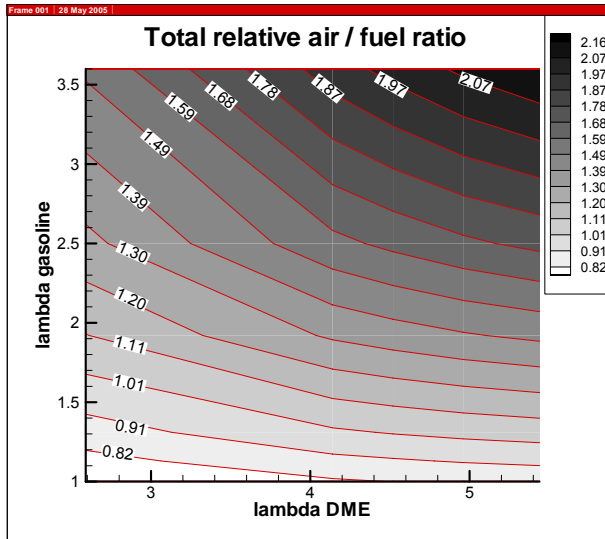


Figure 8 Total relative air / fuel ratio as a function of  $\lambda_{DME}$  and  $\lambda_{gasoline}$

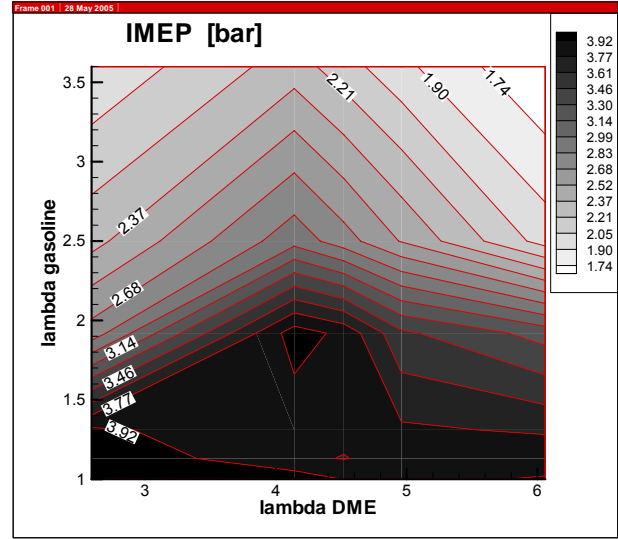


Figure 9 IMEP as a function of  $\lambda_{DME}$  and  $\lambda_{gasoline}$

Figure 9 shows IMEP with respect to the relative air / fuel ratios of gasoline and DME. The horizontal axis represents the relative air / DME ratio, and the vertical axis represents the relative air / gasoline ratio. This shows that the IMEP is influenced by DME and gasoline injection amount. It also shows that there is an optimum amount of DME for best IMEP, which corresponds to the approximate value of 4.2 in the relative air / DME ratio. Misfire and partial burn occurred at the right boundary of the operation region, which is reflected on the lower value of the average IMEP. When relative air / gasoline ratio is lower than 1, severe knock and rapid pressure rise were observed.

Figure 10 shows fuel conversion efficiency with respect to the relative air / fuel ratios of gasoline and DME. When relative air / gasoline ratio is 2 and relative air / DME ratio is 4.2, the best fuel conversion efficiency of 25% was obtained. This high fuel conversion efficiency region is at the same region of high IMEP region as shown in Figure 9.

Figure 11 shows that HC emission is influenced significantly by relative air / gasoline ratio than relative air / DME ratio. Triangular area of the map; relative air / gasoline ratio is 1.5 ~ 3 and relative air / DME ratio is 4.5 ~ 6, HC emission was increased dramatically. This could be attributed to small amount of the injected DME which is not enough to reduce the quenching effect and to enhance the oxidation process at expansion stroke. Out of this triangle area, at lower air / gasoline ratio ( $< 1.7$ ), HC emission was relatively decreased due to the high combustion temperature. However, upper area in the HC emission map, HC emission was increased as relative air / gasoline ratio was increased. This is because of the incomplete combustion with reduction of oxidation amount during expansion stroke.

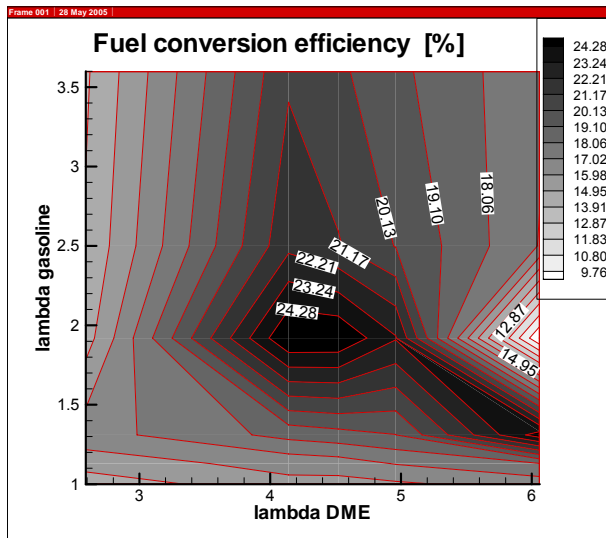


Figure 10 Fuel conversion efficiency as a function of  $\lambda_{DME}$  and  $\lambda_{gasoline}$

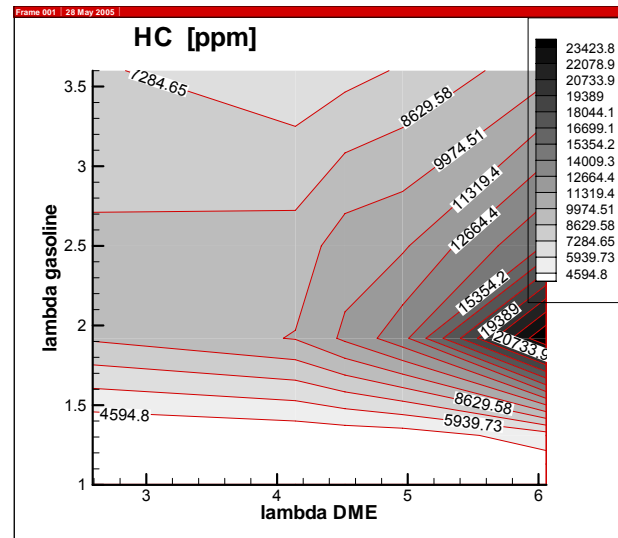


Figure 11 HC emission as a function of  $\lambda_{DME}$  and  $\lambda_{gasoline}$

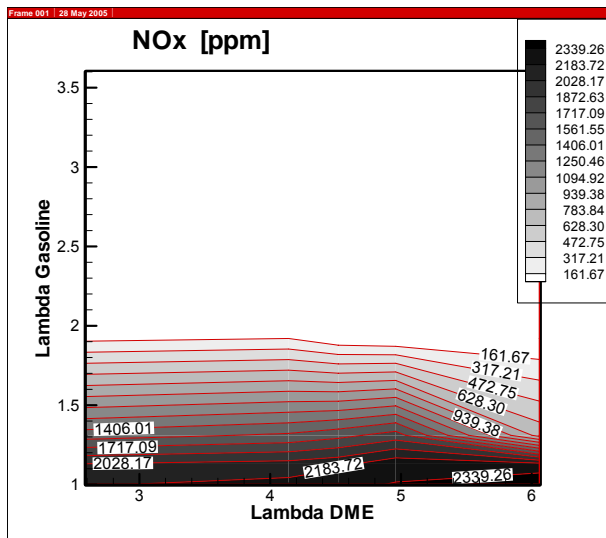


Figure 12 NOx emission as a function of  $\lambda_{DME}$  and  $\lambda_{gasoline}$

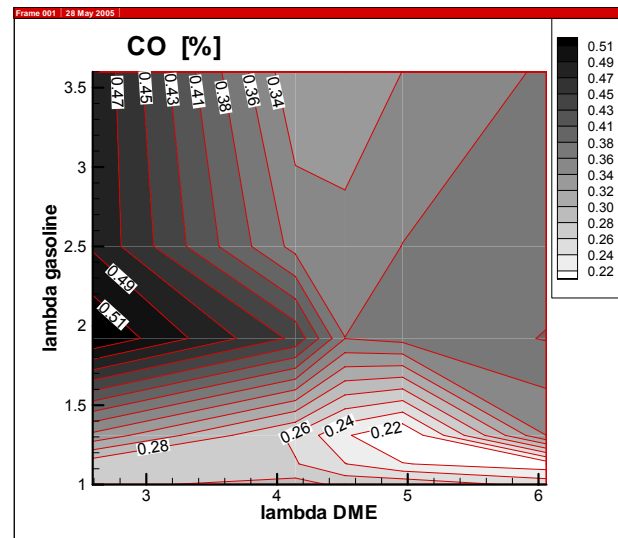


Figure 13 CO emission as a function of  $\lambda_{DME}$  and  $\lambda_{gasoline}$

NOx emission map is shown in Figure 12. One of the major advantages of HCCI engine is ultra low NOx emission [2]. When relative air / gasoline ratio was over 1.7, NOx emission was under 500 ppm. However, relative air / gasoline ratio was decreased to less than 1.7, NOx emission was increased as a result of the vigorous combustion process and the high combustion temperature.

Figure 13 represents the map of CO emission. CO emission is closely related to relative air / fuel ratio of the mixture and oxidation reaction during expansion stroke [12]. At bottom right region of CO emission map, the lowest CO emission region was observed. However, CO emission was increased as relative air / DME ratio was decreased at bottom region of CO emission map. But, CO emission was decreased as relative air / gasoline ratio was decreased at all region of CO emission map. This is because combustion temperature at lower region of CO emission map was higher



than upper region and most of CO emission generated at combustion process could oxidize at expansion stroke.

The effects of wide range of IVO timings, DME injection timings, and fuel quantities were investigated at this work. Combustion pressure and rate of heat release are to be investigated as a function of mixture ratio and valve timings at various engine conditions.

## Conclusions

Gasoline HCCI combustion was controlled by VVT and DME direct injection. The effects of IVO timing and DME direct injection and fuel quantities on HCCI combustion were investigated. Following conclusions were drawn from the experimental results.

1. Ignition delay and rapid burning angle were successfully controlled by the amount of internal EGR that was determined with VVT.
2. For best IMEP and low HC emission, DME should be injected during early compression stroke.
3. IMEP was mainly affected by the DME injection timing, and quantities of fuel; DME and gasoline.
4. HC emission was mainly affected by both the amount of gasoline and the DME injection timing.
5. NO<sub>x</sub> emission was lower than conventional SI engine at gasoline lean region. However, NO<sub>x</sub> emission was similar to that in the conventional SI engine at gasoline rich region.
6. CO emission was affected by the amount of gasoline and DME.

## Acknowledgements

The authors would like to thank CERC (Combustion Engineering Research Center), KAIST and National Research Laboratory scheme for the financial support.

## Literature

- [1] K. Hiraya, K. Hasegawa, T. Urushihara, A. Iiyama, and T. Itoh, "A Study on Gasoline Fueled Compression Ignition Engine ~ A Trial of Operating Region Expansion~", SAE Technical Paper, No. 2002-01-0416, 2002.
- [2] F. Zhao, T. Asmus, D. Assanis, J. Dec, J. Eng, P. Najt, *Homogeneous Charge Compression Ignition (HCCI) Engines : Key Research and Development Issues*, SAE, 2003.
- [3] J. Hyvonen, G. Haraldsson and B. Johansson, "Supercharging HCCI to Extend the Operating Range in a Multi-Cylinder VCR-HCCI Engine", SAE Technical Paper, No. 2003-01-3214, 2003.
- [4] M. Christensen, B. Johansson, P. Amneus and F. Mauss, "Supercharged Homogeneous Charge Compression Engine", SAE Technical Paper, No. 980787, 1998.

- [5] L. Koopmans and I. Denbratt, "A Four Stroke Camless Engine, Operated in Homogeneous Charge Compression Ignition Mode with Commercial Gasoline", SAE Technical Paper, No. 2001-01-3610, 2001.
- [6] J. Allen and D. Law, "Variable Valve Actuated Controlled Auto-Ignition : Speed Load Maps and Strategic Regimes of Operation", SAE Technical Paper, No. 2002-01-0422, 2002.
- [7] P. Wolters, W. Salber, J. Geiger, M. Duwsmann and J. Dilthey, "Controlled Auto Ignition Combustion Process with an Electromechanical Valve Train", SAE Technical Paper, No. 2003-01-0032, 2003.
- [8] J. Hyvonen, G. Haraldsson and B. Johansson, "Operating Range in a Multi Cylinder HCCI Engine Using Variable Compression Ratio", SAE Technical Paper, No. 2003-01-1829, 2003.
- [9] S. Kajitani, C. Chen, M. Oguma, M. Alam and K. Rhee, "Direct Injection Diesel Engine Operated with Propane – DME Blended Fuel", SAE Technical Paper, No. 982536, 1998.
- [10] Z. Chen, M. Konno, M. Oguma, T. Yanai, "Experimental Study of CI Natural-Gas/DME Homogeneous Charge Engine", SAE Technical Paper, No. 2000-01-0329, 2000.
- [11] H. Sandquist, J. Wallesten, K. Enwald and S. Stromberg, "Influence of Valve Overlap Strategies on Residual Gas Fraction and Combustion in a Spark-Ignition Engine at idle", SAE Technical Paper, No. 972936, 1997.
- [12] J. B. Heywood, *Internal Combustion Engine Fundamentals*, Mc Graw Hill, 1988.
- [13] H. Zhao, Z. Peng, J. Williams and N. Ladommatos, "Understanding the Effects of Recycled Burnt Gases on the Controlled Autoignition (CAI) Combustion in Four-Stroke Gasoline Engines", SAE Technical Paper, No. 2001-01-3607, 2001.

## List of Notation

$\lambda_{\text{DME}}$	Relative air/fuel ratio of DME
$\lambda_{\text{gasoline}}$	Relative air/fuel ratio of gasoline

## Abbreviation

AC	Alternating Current
ABDC	After Bottom Dead Center
ATDC	After Top Dead Center
BBDC	Before Bottom Dead Center
BMEP	Brake Mean Effective Pressure
BTDC	Before Top Dead Center
CAD	Crank Angle Degree
CO	Carbon Oxide
CO <sub>2</sub>	Carbon Dioxide
DME	Di-Methyl Ether
DOHC	Double Over Head Camshaft
EGR	Exhaust Gas Recirculation
EMV	Electro Magnetic Valvetrain
HC	Hydro Carbon
HCCI	Homogeneous Charge Compression Ignition
HSDI	High Speed Direct Injection
NO <sub>x</sub>	Nitrogen Oxide and Nitrogen Dioxide
IMEP	Indicated Mean Effective Pressure
PM	Particular Matter
RPM	Revolution Per Minute
TDC	Top Dead Center
VCR	Variable Compression Ratio
VVA	Variable Valve Actuation
VVT	Variable Valve Timing

## Authors

Mr. Kitae Yeom

KAIST

Engine laboratory, Department of Mechanical Engineering

Korea Advanced Institute of Science and Technology

373-1, Guseong-dong, Yuseong-gu, Daejeon, Republic of Korea 305-701

Mr. Jinyoung Jang

KAIST

Engine laboratory, Department of Mechanical Engineering

Korea Advanced Institute of Science and Technology

373-1, Guseong-dong, Yuseong-gu, Daejeon, Republic of Korea 305-701

Dr. Choongsik Bae

KAIST

Associate Professor

Engine laboratory, Department of Mechanical Engineering

Korea Advanced Institute of Science and Technology

373-1, Guseong-dong, Yuseong-gu, Daejeon, Republic of Korea 305-701